JOURNAL OF NANO- AND ELECTRONIC PHYSICS
Vol. **18** No 1, 01003(6pp) (2026)

ЖУРНАЛ НАНО- ТА ЕЛЕКТРОННОЇ ФІЗИКИ
Том **18** № 1, 01003(6cc) (2026)

OPEN ACCESS

REGULAR ARTICLE

Electronic Structure of ZnTS Crystals Modified by the Zn-S Swap Disorder

S.V. Syrotyuk[1,*], A.Y. Nakonechnyi[1], M.K. Hussain[2], S.O. Yuriev[1]

[1] *Lviv Polytechnic National University, 79013 Lviv, Ukraine*
[2] *Department of Electrical Power Techniques Engineering, AL-Hussain University College, 56001 Kerbala, Iraq*

(Received 22 August 2025; revised manuscript received 14 February 2026; published online 25 February 2026)

This work is devoted to the study of changes in the electronic structure of ZnS crystals in the simultaneous presence of two types of defects. The first of them is an impurity of a transition 3d element - Mn or Fe. These impurities replace the Zn atom in the crystal. The second type of structural defects in the crystal is the mutual exchange of positions of Zn and S atoms, i.e. Zn-S swap disorder. The partial densities of states reveal significant differences in the 3d electron densities of Mn and Fe atoms. This results in significant differences in the magnetic moments of the ZnMnS and ZnFeS supercells. If the typical values of the magnetic moments of ZnMnS and ZnFeS supercells are 5 and $4\mu_B$, respectively, then their values in the same materials with the introduced Zn-S swap disorder are 3.1 and $2.3\mu_B$, respectively. The electronic structure of both materials was calculated within the framework of the full electron density functional (DFT) theory using the hybrid exchange-correlation functional PBE0.

Keywords: Cubic ZnS crystal, TM impurity, Swap disorder, Electronic structure, Magnetic moment.

DOI: 10.21272/jnep.18(1).01003 PACS numbers: 71.15.Mb, 71.20.Nr, 71.27. + a

1. INTRODUCTION

Zinc Sulfide (ZnS) thin film has attracted increasing attention due to their potential applications in the new generation of nano-electronics and optoelectronics devices. The physical and chemical properties of ZnS have outstanding quality for different applications. Moreover, ZnS doped with various elements are creating a new era for both academic research and industrial applications. So, the optical properties of modified ZnS thin film will help us to find a suitable doping element for convenient deposition which may enhance the conductance and transmitting properties of the film. This review work has been carried out to explore the four-modification elements that constitute Cu, Ni, Co and Fe as descending order of atomic number corresponding to Zn, along with some potential applications considering the recent research work with other doping elements too such as Al, C, Pt etc. [1]

ZnTS materials, where T is a transition 3d element, are actively studied by theoretical and experimental methods [2]. Native point defects in ZnS were studied within first-principles approaches based on LDA, LDA + U and an extrapolation scheme. First-principles calculations based on LDA, LDA + U and an extrapolation scheme are performed to study the native point defects in zincblende ZnS, and the three methods give similar results. Zinc vacancies in the 2^- charge state have extremely low formation energy at the conduction band minimum (CBM), thus they will heavily compensate the n-type doping of ZnS. In Zn-rich conditions, sulfur antisites and zinc interstitials in the zinc cage sites are compensating centers in p-type ZnS.

Zinc sulphide (ZnS) is considered a viable candidate for light-emitting diodes, electroluminescent devices, flat panel displays, infrared windows, sensors, lasers, and solar cells. Numerous methods, including electrochemical deposition, microemulsion, solvothermal, sol–gel, co-precipitation, combustion synthesis, pyrolysis, hydrothermal, laser ablation, and vapor deposition, have been used to fabricate ZnS nanostructures. The hydrothermal method is adaptable, productive, and able to be adjusted; it doesn't require milling or calcination, has low contamination, and is cost-effective. It also has a high ability to regulate the nucleation process [3].

Customizing the chromatic discharge of nanomaterials is crucial for their use in light-emitting screens, field emitters, lasers, sensors, and optoelectronic devices [4]. ZnS nanocrystals exhibit blue, green, and orange emissions. The luminescence characteristics of ZnS particles have been altered by doping with various transition elements and rare-earth metals. The optical characteristics are affected by defects, crystal structure, size, and shape. These studies show the ability to adjust several emission characteristics from pure ZnS nanocrystals with various defect features. Despite significant efforts to investigate the optical features, the sources of various photoluminescence (PL) bands from ZnS are infrequently addressed. The ZnS luminescence properties are typically attributed to surface states, Sulphur vacancies, Zn vacancies, elemental Sulphur species, or impurities in ZnS [5]. There are many hanging bands and imperfections in the surface of ZnS due to its diverse interface topologies and larger specific surface areas.

* Correspondence e-mail: stepan.v.syrotiuk@lpnu.ua

Cite this article as: N.M. Belyavina et al., *J. Nano- Electron. Phys.* 18 No 1, 01003 (2026) https://doi.org/10.21272/jnep.18(1).01003

The global scarcity of freshwater supplies has long been ingrained in the public's eyes. The world is expected to be water-stressed by 2025 [6]. Water pollution harms the ecosystem balance, so humans will be affected by clean water scarcity shortly. Water-related diseases include communicable diseases (waterborne, water-washed, waterbased, and water-related vector-borne diseases) and noncommunicable diseases caused by chemically polluted water. According to Hermabessiere et al., many plastics in the water are hazardous to a broad spectrum of organisms. Several diseases are caused by chemical waste, including anemia, low blood platelets, headaches, cancer risk, and various skin problems. Semiconductor photocatalysis is the most promising and successful approach for competing with water contaminants. ZnS is an important semiconductor photocatalyst in the II-VI group. ZnS is only sensitive to UV light absorption because of its broad bandgap energy.

The development of visible-light-active photocatalysts capable of utilizing the greatest amount of solar light is an intriguing research area. It is still challenging to improve visible photocatalytic activity by improving charge transfer and efficient charge separation. The other hurdles in this field are low photocatalytic efficiency for visible-light photocatalysts, low mobility of charge carriers, inferior stability of photocatalyst, high recombination rate of electron–hole pairs and cost-effectiveness at the commercial level. The primary disadvantage of ZnS catalysts is their irreversible agglomeration during the photocatalytic processes and limited recyclability, which reduces the photocatalytic degradation efficiency [7].

Defect engineering is another promising method for improving light harvesting in PC materials. Semiconductor photocatalyst defects can function as adsorption sites for charge transfer that prevent the recombination of photoinduced charge and add new energy levels to narrow the band gap that creates visible-light activity. By creating additional energy levels to photoexcited charge carriers' electronic structure and characteristics, vacancy defects can significantly alter the PC activity of a photocatalyst. Doping is also an effective strategy for inducing these defects. The visible light photocatalysis of ZnS has been reported to be improved by the addition of extrinsic metal elements such as Copper, Nickel, Cadmium, or nonmetal elements Carbon and Nitrogen. The inherent characteristics of materials, such as crystalline phases, defect states, exposed facets, etc., of semiconductor photocatalysts are crucial for superior photocatalytic (PC) activities [8].

Simple hydrothermal method for introducing S and Zn vacancies into the ZnS structure is achived by changing the S/Zn molar ratios. Investigations are made into how vacancy-related features affect the photoluminescence and PC activity of ZnS in visible light [9].

Peculiarities of the impact of transition elements on the electronic structure of wide-gap cubic crystals were studied in works [10-14].

However, there are very few publications dedicated to the electronic structure of the materials ZnTS, containing the Zn-S swap disorder defect. That is why the purpose of this study is to identify the changes in the electronic structure of the materials T:ZnS caused by impurities of transition elements T and defects mentioned above.

The problem of calculating the electronic structure of the crystal ZnS with an admixture of Mn and Fe and also with and Zn-S swap disorder defect is relevant, and we proceed to its solution.

2. CALCULATION

The electronic structure of the supercells $Zn_{31}Mn_1S_{32}$ and $Zn_{31}Fe_1S_{32}$ has been evaluated by means of the Abinit [15] code. Calculations of the electronic structure were performed here on the PAW (projector augmented waves) basis [16]. The PAW approach has common features with pseudopotential and full potential methods.

The calculation scheme in the PAW formalism is completed by obtaining an all-electronic wave function $|\psi_{\alpha\mathbf{k}}>$. The latter is derived from the smooth pseudo-wave function of the state $|\tilde{\psi}_{\alpha\mathbf{k}}>$. Here α is a band index, and $\mathbf{k}$ is a vector from the first Brillouin zone. The true all-electronic wave function $|\psi_{\alpha\mathbf{k}}>$ is derived by acting of the operator τ on the smooth pseudo-wave function $|\tilde{\psi}_{\alpha\mathbf{k}}>$ [16],

$$|\psi_{\alpha\mathbf{k}}>=\tau|\tilde{\psi}_{\alpha\mathbf{k}}>. \quad (2)$$

The operator τ is buit on the free atom solutions. In particular, these functions are partial atomic waves φ, pseudowaves $\tilde{\varphi}_i$ and projectors $\tilde{p}_i$. So, the operator τ is defined on these states and has the following form [16]:

$$\tau = 1 + \sum_i (|\varphi_i> - |\tilde{\varphi}_i>) < \tilde{p}_i|. \quad (3)$$

The effective Hamiltonian H_{eff} is derived from the all electron Hamiltonian H by means the similarity transformation, based on a τ operator, namely

$$H_{eff} = \tau^+ H \tau. \quad (4)$$

The pseudowave function $|\tilde{\psi}_{\alpha\mathbf{k}}>$ is the eigenstate of the H_{eff} operator, namely:

$$H_{eff}|\tilde{\psi}_{\alpha\mathbf{k}}>=\tau^+\tau|\tilde{\psi}_{\alpha\mathbf{k}}>\varepsilon_{\alpha\mathbf{k}}. \quad (5)$$

The energy eigenvalues $\varepsilon_{\alpha\mathbf{k}}$, derived from the system of linear equations (5), are identical to those evaluated from the all electron Hamiltonian H:

$$H|\psi_{\alpha\mathbf{k}}>=\varepsilon_{\alpha\mathbf{k}}|\psi_{\alpha\mathbf{k}}>. \quad (6)$$

Having the all-electronic wave function $\psi_{\alpha\mathbf{k}}$, we can calculate the matrix elements of dipole transi-

tions $\mathbf{d}_{fi} = \int \psi_f^* \sum_j e_j \mathbf{r}_j \psi_i d\tau$ necessary to evaluate the optical properties of materials [17], the transport coefficients of semiconductors [18], as well as the Stark effect [19].

The 3d electrons of the Mn or Fe atom move in narrow energy bands and are characterized by large effective mass values. This means that the usual exchange-correlation functional PBE [20], which takes into account the gradient corrections of the electron density, is not suitable for an adequate description of 3d electrons. That is why we use the hybrid exchange-correlation functional PBE0 here. The latter is employed in the following form [21], namely

$$E_{xc}^{PBE0}[\rho] = E_{xc}^{PBE}[\rho] + \beta(E_x^{HF}[\Psi_{3d}] - E_x^{PBE}[\rho_{3d}]) \quad (7)$$

In this functional, the exchange-correlation energy of the 3d electrons of the transition element E_x^{PBE}, found in the GGA approximation, is partially removed, and the exchange energy of the same electrons, found in the Hartree-Fock theory E_x^{HF}, is substituted in its place.

Namely, the PBE0 functional is a mixture of two exchange-correlation functionals. The first of them is the usual GGA functional. It is suitable for smoothly varying electron densities in space. The second term in Eq. (5) contains the Hartree-Fock energy, in which there is no self-interaction error, which is very large for electrons that move in narrow energy bands, namely 3d electrons. The mixing factor β is recommended to be 0.25 [21].

3. RESULTS AND DISCUSSION

All results presented in figures 1-5 were obtained using the Abinit software package. The electronic energy spectra and densities of electronic states were modified by two types of defects in the ZnS crystal structure, namely the impurity of the transition element T (Mn or Fe) and the mutual exchange of atomic positions in the cell, i.e. a Zn-S swap disorder.

The electronic energy spectra of electrons with spins up and down are shown in Figures 1 and 2, respectively. As can be seen from Figures 1 and 2, the Fermi level intersects the electron energy dispersion curves, which are caused by structural defects in the ZnS crystal. It is worth noting that ZnFeS material without Zn-S swap disorder defects reveals the semiconductor for the majority spins, and the metallic properties for minority spins, showing the supercell magnetic moment of 4 μ_B [11].

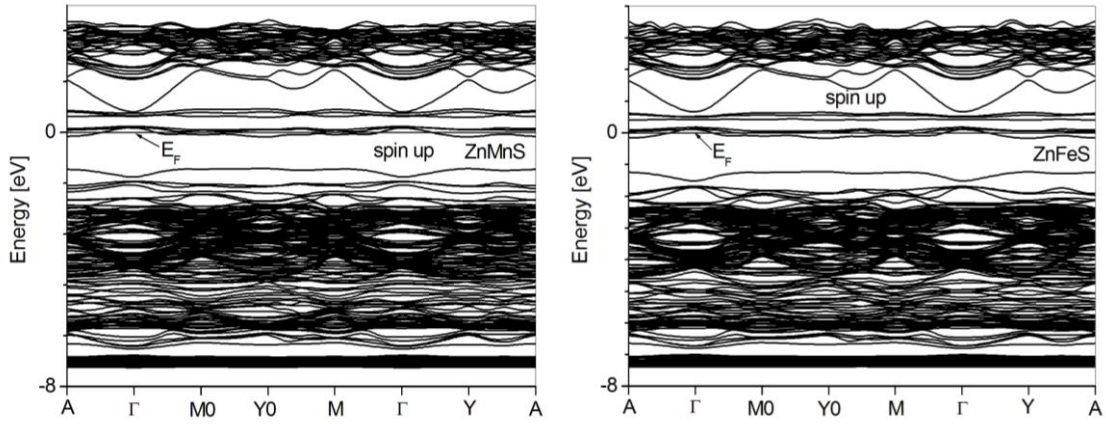

Fig. 1 – The spin up electronic energies evaluated for the supercells $Zn_{31}T_1S_{32}$ (T = Mn, Fe) with the Zn-S swap disorder

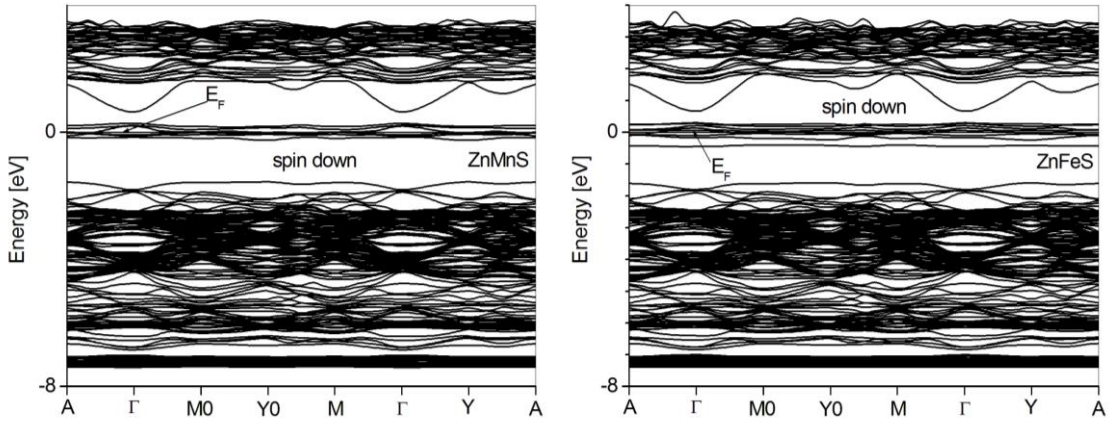

Fig. 2 – The spin down electronic energies evaluated for the supercells $Zn_{31}T_1S_{32}$ (T = Mn, Fe) with the Zn-S swap disorder

And the solid solution of ZnSeS with an admixture of Mn atoms is a semiconductor for both spin moment orientations, having the supercell magnetic moment of 5 μ_B [13].

Comparison of the dispersion curves showed in Figures 1 and 2 reveals only small differences between them. Analysis of the densities of electronic states given in Figures 3-5 reveals the nature of the population of the energy levels.

Curves in Fig. 3 reveal a significant asymmetry of the Mn or Fe d states, which indicates the presence of a non-zero magnetic moment of the supercell. For the supercell ZnMnS the total magnetic moments equals to 3.1 μ_B, and the contribution of Mn atom equals to 3.8 μ_B. For the supercell ZnFeS the total magnetic moments equals to 2.3 μ_B, and the contribution of Fe atom equals to 3.4 μ_B. Therefore, the numerical values of the magnetic moments localized on the Mn and Fe atoms are 3.8 and 3.4 μ_B, respectively. However, the magnetic moments of the ZnMnS and ZnFeS supercells are significantly smaller, and equal to 3.1 and 2.3 μ_B, respectively. This is a rather unexpected result. What is the reason for this phenomenon? So, there must be some fraction of atoms in the supercells that acts in the antiferromagnetic mode with the Mn and Fe impurities present in them. We found the answer to this intriguing question, and its essence is as follows. The greatest opposition to the magnetic moments of Mn and Fe atoms arises from the side of S atoms. The greatest values are exhibited by S atoms, which are participants in the formation of the Zn-S swap disorder defect. The values of the opposing magnetic moments on these S atoms, which are located in the ZnMnS and ZnFeS supercells, are as follows: -0.325 and -0.305 μ_B, respectively.

The partial densities of states on Zn and S atoms, presented in Fig. 4, show that the valence band is formed mainly by S p-states. However, Zn atoms mainly delegate s states to the conduction zone.

We also note in Fig. 3 narrow energy bands of d symmetry in the valence band, which are characterized by large values of the density of electronic states. For an adequate description of such states, we employ the PBE0 hybrid exchange-correlation functional (5). The usual GGA functional is unsuitable for describing electrons moving in narrow energy bands of d symmetry.

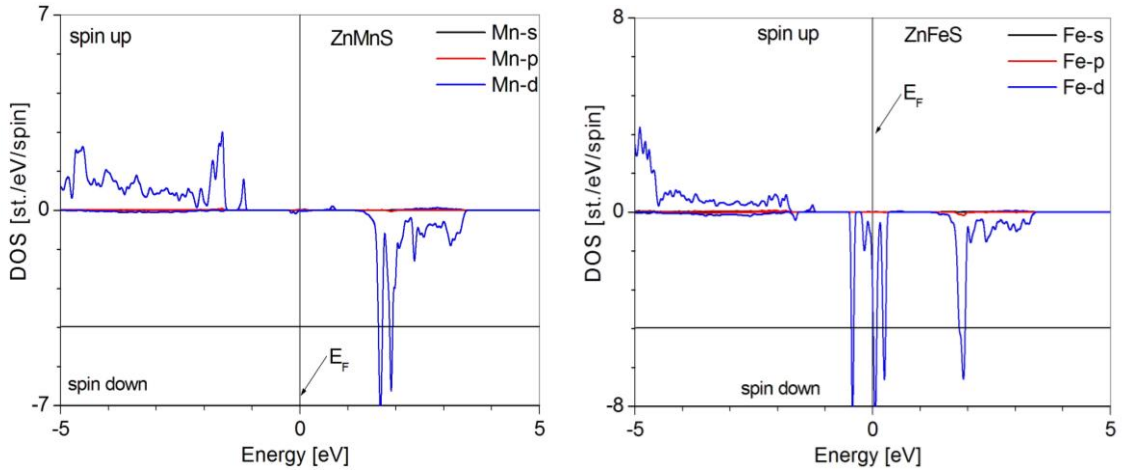

Fig. 3 – The spin-resolved partial DOS, evaluated for the supercells $Zn_{31}T_1S_{32}$ (T = Mn, Fe), with the Zn-S swap disorder

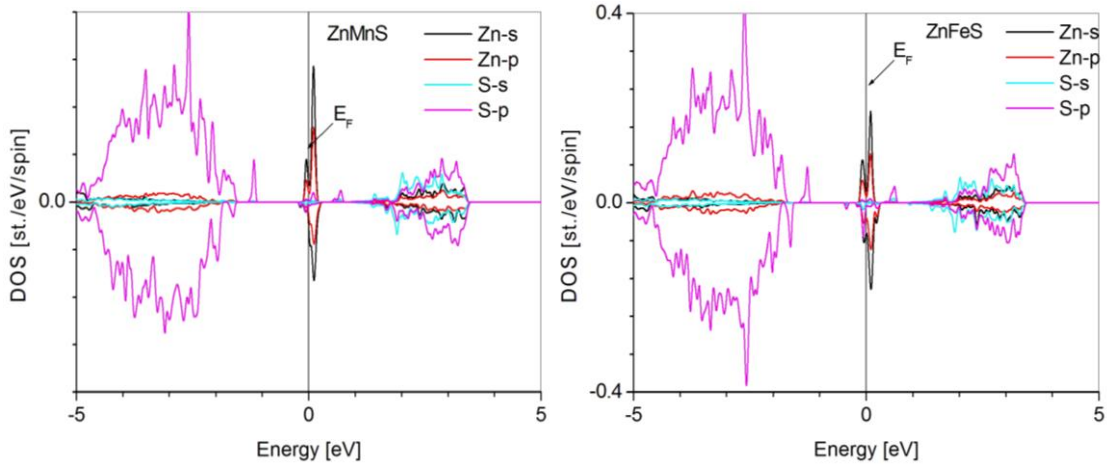

Fig. 4 – The spin-resolved partial DOS, evaluated for the supercells $Zn_{31}T_1S_{32}$ (T = Mn, Fe), with the Zn-S swap disorder

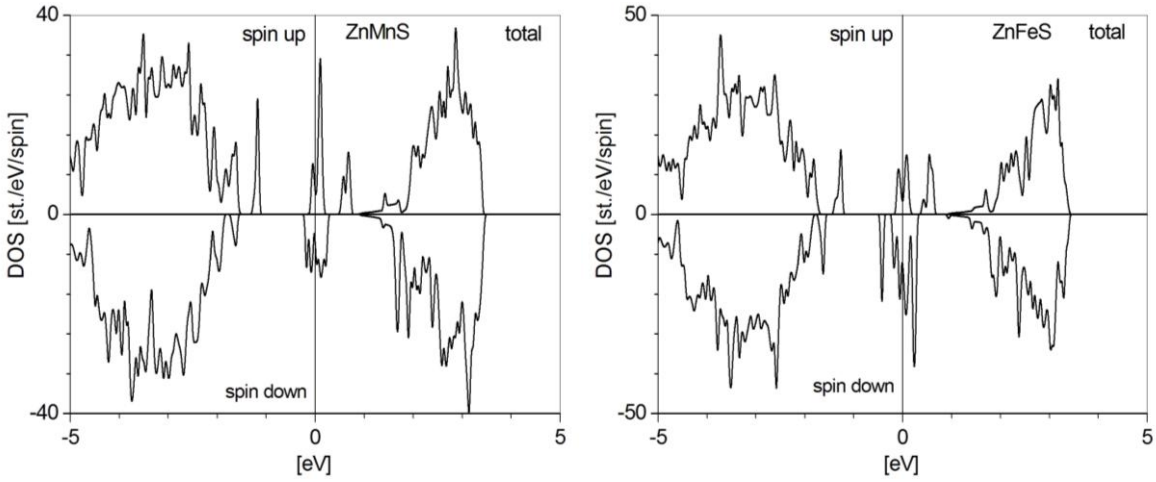

Fig. 5 – The spin-resolved total DOS, evaluated for the supercells $Zn_{31}T_1S_{32}$ (T = Mn, Fe), with the Zn-S swap disorder

It is these charge carriers that are characterized by a large amount of self-interaction energy, partially excluded in the PBE0 functional. The asymmetry of the partial DOS curves, as well as the total density of electronic states (Fig. 5), is the result of the influence of the transition elements Mn or Fe on the polarization of the electron density, even on such non-magnetic element as S.

4. CONCLUSIONS

The spin-polarized electronic structure of the Mn:ZnS and Fe:ZnS materials, where the Zn is replaced by the Mn or Fe atom, is investigated. Electronic energy bands were evaluated for $Zn_{31}Mn_1S_{32}$ and $Zn_{31}Fe_1S_{32}$ supercells with the Zn-S swap disorder. The Zn-S swap disorder causes significant changes in the electronic structure of the ZnTS materials. The ZnMnS material is a semiconductor for both spin orientations, and ZnFeS is a semimetal, but both of these materials exhibit metallic nature in the presence of Zn-S swap disorder.

ACKNOWLEDGEMENTS

This contribution was created under the support of the High Performance Computing Laboratory at the Lviv Polytechnic National University.

REFERENCES

1. A.M. Shakil, S. Das, A.M. Rahman, U.S. Akther, K.M.H. Majumdar, K.M. Rahman, *Mater. Sci. Appl.* **9**, 751 (2018).
2. P. Li, S. Deng, L. Zhang, G. Liu, J. Yu, *Chem. Phys. Lett.* **531**, 75 (2012).
3. E.M. Jubeer, M.A. Manthrammel, P.A. Subha, M. Shkir, K.P. Biju, S.A. AlFaify, *Sci. Rep.* **13**, 16820 (2023).
4. F.H. Su, Z.L. Fang, B.S. Ma, K. Ding, G.H. Li, S.J. Xu, *J. Appl. Phys.* **95**, 3344 (2004).
5. X. Wang, J. Shi, Z. Feng, M. Li, C. Li, *Phys. Chem. Chem. Phys.* **13**, 4715 (2011).
6. B.D. Deshpande, P.S. Agrawal, M.K.N. Yenkie, S.J. Dhoble, *Nano-Struct. Nano-Objects* **22**, 100442 (2020).
7. G.J. Lee, J.J. Wu, *Powder Technol.* **318**, 8 (2017).
8. Sharma, K.K. Sharma, P. Raizada, V. Hasija, P. Singh, A. Bajpai, V.-H. Nguyen, S. Rangabhashiyam, P. Kumar, A.K. Nadda, S.Y. Kim, R.S. Varma, T.T.N. Le, Q.V. Le, *J. Water Process Eng.* **43**, 102217 (2021).
9. X. Zhou, Q. Yang, H. Wang, F. Huang, J. Zhang, S. Xu, *J. Mater. Sci. Mater. Electron.* **30**, 1089 (2019).
10. S.V. Syrotyuk, O.P. Malyk, *J. Nano- Electron. Phys.* **11** No 1, 01009 (2019).
11. S.V. Syrotyuk, *J. Nano- Electron. Phys.* **13** No 5, 05027 (2021).
12. S.V. Syrotyuk, M.K. Hussain, *J. Nano- Electron. Phys.* **15** No 5, 05002 (2023).
13. S.V. Syrotyuk, A.Y. Nakonechnyi, Yu.V. Klysko, M.V. Stepanyak, V.M. Myshchyshyn, *J. Nano- Electron. Phys.* **16** No 5, 05033 (2024).
14. S.V. Syrotyuk, A.Y. Nakonechnyi, Yu.V. Klysko, Z.E. Veres, I.I. Lahun, *J. Nano- Electron. Phys.* **16** No 1, 01016 (2024).
15. X. Gonze, F. Jollet, F. Abreu Araujo, D. Adams, B. Amadon, T. Applencourt, C. Audouze, J.-M. Beuken, J. Bieder, A. Bokhanchuk, E. Bousquet, F. Bruneval, D. Caliste, M. Cote, F. Dahm, F. Da Pieve, M. Delaveau, M. Di Gennaro, B. Dorado, C. Espejo,G. Geneste, L. Genovese, A. Gerossier, M.Giantomassi, Y. Gillet, D.R. Hamann, L. He, G. Jomard, J. Laflamme Janssen, S. Le Roux, A. Levitt, A. Lherbier, F. Liu, I. Lukacevic, A. Martin, C. Martins, M.J.T. Oliveira, S. Ponce, Y. Pouillon, T. Rangel, G.-M. Rignanese, A.H. Romero, B. Rousseau, O. Rubel, A.A. Shukri, M. Stankovski, M. Torrent, M.J. Van Setten, B. Van Troeye, M.J. Verstraete, D. Waroquier, J. Wiktor, B. Xu, A. Zhou, J.W. Zwanziger, *Comput. Phys. Commun.* **205**, 106 (2016).
16. P.E. Blöchl, *Phys. Rev. B* **50**, 17953 (1994).
17. Ya. M. Chornodolskyy, V.O. Karnaushenko, V.V. Vistovskyy, S.V. Syrotyuk, A.V. Gektin, A.S. Voloshinovskii, *J. Lumin.* **237**, 118147 (2021).
18. O.P. Malyk, S.V. Syrotyuk, *J. Nano- Electron. Phys.* **14**, 01014 (2022).
19. I.O. Vakarchuk, *Quantum Mechanics* (Ivan Franko National University: Lviv: 2012).
20. J.P. Perdew, K. Burke, M. Ernzerhof, *Phys. Rev. Lett.* **77**, 3865 (1996).
21. F. Tran, P. Blaha, K. Schwarz, P. Novák, *Phys. Rev. B* **74**, 155108 (2006).

Електронна структура кристалів ZnTS, модифікована обміном місцями атомів Zn та S

С.В. Сиротюк[1], А.Й. Наконечний[1], M.K. Hussain[2], С.О. Юр'єв[1]

[1] *Національний університет «Львівська політехніка», 79013 Львів, Україна*
[2] *Department of Electrical Power Techniques Engineering, AL-Hussain University College, 56001 Kerbala, Iraq*

Ця праця присвячена вивченню змін електронної структури кристалів ZnS за одночасної присутності двох типів дефектів. Перший з них – це домішка перехідного 3d-елемента – Mn або Fe. Ці домішки заміщують атом Zn у кристалі. Другий тип структурних дефектів у кристалі – це взаємний обмін місцями атомів Zn та S, тобто локалізаційний безлад Zn-S. Парціальні густини 3d-електронів атомів Mn та Fe виявляють суттєві відмінності. Це приводить до суттєвих відмінностей у магнітних моментах суперемірок ZnMnS та ZnFeS. Якщо типові значення магнітних моментів суперемірок ZnMnS та ZnFeS становлять 5 та $4\mu_B$ відповідно, то їхні значення в тих самих матеріалах із уведеною безладною координацією атомів Zn та S становлять 3,1 та $2{,}3\mu_B$ відповідно. Електронну структуру обох матеріалів було розраховано в рамках теорії повного функціоналу електронної густини (DFT) з використанням гібридного обмінно-кореляційного функціоналу PBE0.

Ключові слова: Кубічний кристал ZnS, Домішка TM, Обміну місцями Zn-S, Електронна структура, Магнітний момент.